Modeling of Enzymatic Reactions in Vesicles: The Case of α-Chymotrypsin

Markus Blocher,[1] Peter Walde,[1] Irving J. Dunn[2]

[1]Institut für Polymere, ETH-Zentrum, Universitätstrasse 6, CH-8092 Zürich, Switzerland; telephone: +41-1-632 3114; fax: +41-1-632 1073; e-mail: walde@ifp.mat.ethz.ch
[2]Industrial Chemistry and Chemical Engineering, ETH-Zentrum, Universitätstrasse 6, CH-8092 Zürich, Switzerland

Received 5 February 1998; accepted 19 June 1998

Abstract: The kinetic behavior of the α-chymotrypsin-catalyzed hydrolysis of the two *p*-nitroanilide substrates succinyl-L-Ala-L-Ala-L-Pro-L-Phe-*p*-nitroanilide (Suc-Ala-Ala-Pro-Phe-pNA) and benzoyl-L-Tyr-*p*-nitroanilide (Bz-Tyr-pNA) was modeled and simulated for two different systems, namely for an aqueous solution and for a vesicle system, which was composed of phospholipid vesicles containing entrapped α-chymotrypsin. In the case of the vesicles, the substrate was added to the bulk, exovesicular aqueous phase. The experimentally determined time-dependence of product (*p*-nitroaniline) formation was modeled by considering the kinetic behavior of the enzyme and—in the case of vesicles—the substrate permeability across the bilayer membrane. In aqueous solution—without vesicles—the kinetic constants k_{cat} and K_S (respectively K_M) were determined from fitting the model to experimental data of batch product concentration–time curves. The results were in good agreement with the corresponding values obtained from initial velocity measurements. For the vesicle system, using the phospholipid 1-palmitoyl-2-oleoyl-*sn*-glycero-3-phosphocholine (POPC), simulation showed that the substrate permeation across the bilayer was rate limiting. Using experimental data, we could obtain the substrate permeability coefficient for Bz-Tyr-pNA by parametric fitting as 2.45×10^{-7} cm/s. © 1999 John Wiley & Sons, Inc. *Biotechnol Bioeng* **62:** 36–43, 1999.
Keywords: liposomes; vesicles; microreactor; modeling; permeability; chymotrypsin; enzyme

INTRODUCTION

Recently, the catalytic activity of the water soluble proteolytic enzyme α-chymotrypsin entrapped inside lipid vesicles (liposomes) was investigated (Walde and Marzetta, 1998). The vesicles were composed of 1-palmitoyl-2-oleoyl-*sn*-glycero-3-phosphocholine (POPC), and it was in particular demonstrated that the entrapped enzyme showed a pronounced selectivity towards externally added substrates. While the hydrolysis of small and uncharged substrates like benzoyl-L-Tyr-p-nitroanilide (Bz-Tyr-pNA) was catalyzed by the entrapped α-chymotrypsin, the hydrolysis of larger substrates such as succinyl-L-Ala-L-Ala-L-Pro-L-Phe-*p*-nitroanilide (Suc-Ala-Ala-Pro-Phe-pNA) was not. This experimental finding was interpreted qualitatively on the basis of differences in the permeability properties of the vesicles for the two types of substrates. Bz-Tyr-pNA could migrate from the bulk aqueous medium across the bilayer shell of the vesicle microreactor into the vesicle's aqueous interior, where α-chymotrypsin catalyzed the hydrolysis reaction (see Fig. 1). On the other hand, Suc-Ala-Ala-Pro-Phe-pNA could not reach the entrapped enzyme, since it could not permeate across the phospholipid bilayer under the conditions used. We therefore concluded that the observed substrate selectivity of α-chymotrypsin was based entirely on the compartmentalization and permeability properties of the liposome microreactor system. Similarly, the rates of amino acid oxidation in a system containing liposome-entrapped D-amino acid oxidase were analyzed by assuming that the rate-limiting step in the reaction was the transport of the amino acid across the liposome bilayer and that all the amino acids reacted with identical enzyme kinetics (Naoi et al., 1977).

In an extension of our work on α-chymotrypsin, we now report on a series of new experiments with the aim of obtaining quantitative information on the permeability coefficient of the selected substrate for the vesicles used. This is accomplished by modeling the experiments and fitting the parameter to the data. Since the substrate concentration in the system used was not in excess with respect to the endovesicular enzyme concentration, the simple Michaelis–Menten equation could not be applied (see below).

Quite generally, enzyme-containing vesicles are interesting systems in which a biocatalyst is immobilized noncovalently, and potential applications in drug delivery have been discussed (Torchilin, 1987; Scheper, 1990). Furthermore, a quantitative understanding of enzymatic reactions in vesicles is important if enzyme-containing vesicles are considered as bioanalytical tools (Rosenberg et al., 1991). One may also consider that enzyme-containing vesicles could be used for biospecific reactions, using substrate mixtures: only those substrates for which the vesicle membrane is permeable would be converted.

Correspondence to: P. Walde

 CCC 0006-3592/99/010036-08

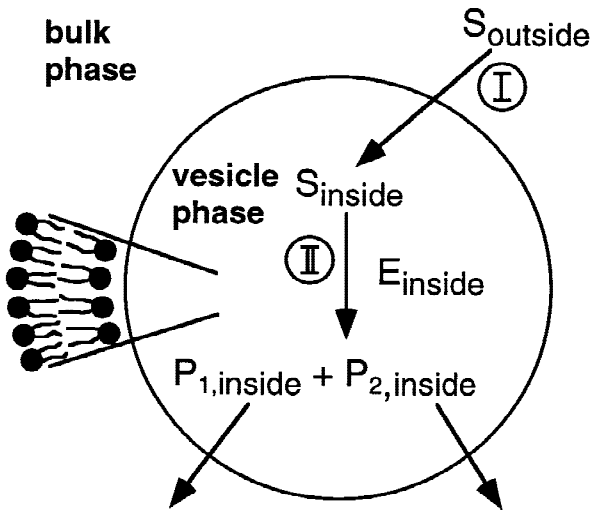

Figure 1. Schematic representation of the vesicle system used, showing a cross-section through one single vesicle of radius R_v, containing α-chymotrypsin which catalyzes the transformation of substrate S into the two products, P_1 and P_2, inside the vesicles. The main processes considered are the diffusion of S from the bulk phase across the vesicle bilayer (I), described by Eq. (6), and the enzyme-catalyzed hydrolysis reaction (II), described by Eq. (5).

MATERIALS AND METHODS

Chemicals

POPC was a gift from the Pharma Research Department of Novartis International Ltd., Basel, Switzerland. Bovine pancreatic α-chymotrypsin and bovine pancreatic trypsin inhibitor (abbreviated as BPTI; commercial name Aprotinin) were from Fluka, Buchs, Switzerland. $CaCl_2 \cdot 2H_2O$ was from Sigma, Buchs, Switzerland, and all other chemicals used were commercially available as described before (Walde and Marzetta, 1997).

Preparation of α-Chymotrypsin-Containing Vesicles

Vesicles were prepared from POPC because it is a welldefined, naturally occurring phospholipid, commercially available in large quantities and in pure form. At room temperature, POPC bilayers are in the fluid-analogue state since the phase transition temperature is at −3°C (Lynch and Steponkus, 1989). POPC vesicles containing entrapped α-chymotrypsin were prepared by the so-called extrusion method, followed by a separation of the nonentrapped enzyme from the α-chymotrypsin-containing vesicles by gel permeation chromatography: 45 mg POPC (=59 μmol) were first dissolved in 3 mL $CHCl_3$ in a 50 mL round-bottom flask. After evaporation of the solvent by rotatory evaporation under reduced pressure, the thin film was dried during 1 day at high vacuum. The POPC was then dispersed at room temperature by adding 3 mL 50 m*M* Tris/HCl, pH 8, containing 60 mg α-chymotrypsin (from bovine pancreas). Vortexing helped to speed up the dispersion process which led to the formation of mainly multilamellar vesicles with a considerable size heterogeneity (Bangham et al., 1965; Papahadjopoulos and Kimelberg, 1974). The vesicle suspension was then repetitively frozen in liquid nitrogen and thawed in a water bath at 25°C (10 times) in order to homogenize the distribution of α-chymotrypsin between the interior of the vesicles and the bulk aqueous phase (Mayer et al., 1985). During these freeze–thaw cycles, the size of the vesicles may change, thereby reducing the number of small unilamellar vesicles and increasing the content of multivesicular vesicles, nonconcentric vesicles within vesicles (e.g. Anzai et al., 1990; Hope et al., 1993). A significant decrease in size and lamellarity was achieved by repetitively passing the vesicle suspension through Nucleopore polycarbonate membranes with mean pore diameters of 400 nm (10 times), 200 nm (10 times), and 100 nm (10 times), using The Extruder from Lipex Biomembranes Inc., Vancouver, Canada (Hope et al., 1993). After this so-called extrusion procedure, the vesicles containing α-chymotrypsin were separated from free enzyme chromatographically on Sepharose 4B (from Pharmacia Biotech, Dübendorf, Switzerland), packed in a column 45 cm in length and 1.6 cm in diameter, by applying 1 mL of the extruded vesicle suspension. Elution was performed with 50 m*M* Tris/HCl, pH 8, at a speed of 0.5 mL/min (with a P-3 peristaltic pump from Pharmacia Biotech, Dübendorf, Switzerland), collecting fractions of 2 mL. The optical density of each fraction was then measured by using quartz cells with 1 cm path length at 280 nm (absorption maximum of α-chymotrypsin and light scattering due to the presence of the vesicles). The chromatogram shown in Fig. 2 indicates that the nonentrapped α-chymotrypsin (peak 2) could well be separated from the vesicles (peak 1). Fractions 14–20, corresponding to an elution volume of 28–40 ml were pooled, stored at 4°C, and further characterized and used for the kinetic measurements.

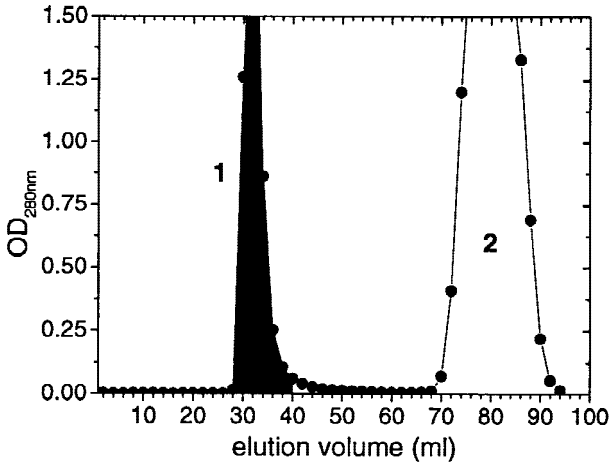

Figure 2. Gel permeation chromatographic separation of α-chymotrypsin-containing vesicles (peak 1) from nonentrapped α-chymotrypsin (peak 2). For details see ''Materials and Methods.'' The pooled fractions are marked in black.

Characterization of α-Chymotrypsin-Containing Vesicles

The POPC concentration in the pooled vesicle sample was determined by using the Stewart assay, in which the phospholipids are quantified colorimetrically after complexation in chloroform with ammonium ferrothiocyanate (Stewart, 1980). α-Chymotrypsin was quantified with an activity assay, using Suc-Ala-Ala-Pro-Phe-pNA (initial concentration 25 μ*M*; Bru and Walde, 1991; DelMar et al., 1979) after destroying the vesicles with sodium cholate at a concentration of 40 m*M*. An appropriate calibration curve (containing 40 m*M* cholate) was applied with known amounts of α-chymotrypsin. The absolute concentration of active enzyme was determined with *N-trans*-cinnamoylimidazole as described before (Schonbaum et al., 1961). For the α-chymotrypsin used in this study, an enzyme purity of 73% was determined. For all data presented in this work, the concentration of α-chymotrypsin as obtained by this active site titration was taken into account.

The mean size of the α-chymotrypsin-containing vesicles of diluted samples (1:1 v/v, diluted with 50 m*M* Tris/HCl, pH 8) was determined by dynamic light scattering measurements as described before (Walde and Marzetta, 1998).

Electron micrographs were taken by using the freeze–fracture method (Müller et al., 1980) and by using the cryo-immobilization technique (Egelhaaf et al., 1996).

Kinetic Measurements

The rate of hydrolysis of Bz-Tyr-pNA or Suc-Ala-Ala-Pro-Phe-pNA was followed at 25°C by monitoring the increase in optical density at 410 nm as a function of time by using 1 cm quartz cells and a Cary 1E UV/visible spectrophotometer (from Varian International AG, Basel, Switzerland). In a typical experiment, 65 μL of a α-chymotrypsin-containing vesicle sample ([POPC] = 1.3 m*M*; $[\alpha\text{-chymotrypsin}]_{overall}$ = 860 n*M*; 50 m*M* Tris/HCl, pH 8) and 815 μL 50 m*M* Tris/HCl, pH 8, were first incubated with 50 μL 0.1 m*M* BPTI solution (in 50 m*M* Tris/HCl, pH 8) for 5 min at 25°C. The reaction was started by adding 70 μL 1.5 m*M* Bz-Tyr-pNA (dissolved in dimethyl sulfoxide). The molar extinction coefficient of *p*-nitroaniline at 410 nm was 8800 M^{-1} cm^{-1} (Mao and Walde, 1991). For the dynamic modeling and parameter estimation, the reaction was generally followed until equilibrium (100% hydrolysis).

Dynamic Simulation

For simulation and parameter estimation, the software ''ModelMaker'' from Cherwell Scientific Publishing Ltd, Oxford (U.K.), was used.[1] Numerical integrations and optimizations were performed with the implemented Runge–Kutta method (fourth order) and with the Marquardt algorithm, respectively.

[1] Refer to http://www.cherwell.com.

MODELING AND THEORETICAL ASPECTS

α-Chymotrypsin Kinetics in the Absence of Vesicles

The kinetic analysis used in the present work is related to Scheme 1 developed for the α-chymotrypsin-catalyzed hydrolysis of esters and amides (e.g. Fersht, 1985),

$$E + S \underset{k_{-1}}{\overset{k_1}{\rightleftharpoons}} ES \overset{k_2}{\rightarrow} EP' \overset{k_3}{\rightarrow} E + P_2 + P_1 \quad \text{(Scheme 1)}$$

where k_1 and k_{-1} are the rate constants for the formation and dissociation of the enzyme–substrate complex (ES), respectively; k_2 and k_3 are the rate constants for the decompositions of ES and EP′ (the acylenzyme intermediate) to yield the two products P_1 and P_2 and free enzyme (E). The turnover number (k_{cat}) is related to k_2 and k_3 through Eq. (1) by applying the steady-state assumption for EP′,

$$k_{cat} = \frac{k_2 k_3}{k_2 + k_3}, \tag{1}$$

and the velocity (v) depends then on the substrate concentration as in the well-known Briggs–Haldane equation, Eq. (2), also known as the Michaelis–Menten equation,

$$v = \frac{k_{cat}[E]_t[S]}{K_M + [S]}, \tag{2}$$

where $[E]_t$ corresponds to the total enzyme concentration (e.g. Fersht, 1985; Segel, 1975). For Scheme 1 K_M is still called the Michaelis constant but is now defined as

$$K_M = K_S \frac{k_3}{k_2 + k_3} \tag{3}$$

and

$$K_S = \frac{[E][S]}{[ES]} = \frac{k_{-1}}{k_1}. \tag{4}$$

Since in the case of amide substrates—as used in the present work—acylation is rate limiting ($k_2 << k_3$), it follows from Eq (1) and (3) that $k_{cat} \cong k_2$ and $K_M \cong K_S$ (Fersht, 1985).

For Eq. (2) and the conventional Michaelis–Menten equation, it is assumed that the total substrate concentration is much larger than the total enzyme concentration, $[S]_{tot} >> [E]_{tot}$. If this is not the case—as in the aqueous interior of the α-chymotrypsin-containing vesicles used in the present study—the more general expression, Eq. (5), for the Michaelis–Menten scheme should be used (Keleti, 1986; Segel, 1975):

$$v = \frac{k_2}{2}\left[([E]_{tot} + [S]_{tot} + K_S) - \sqrt{([E]_{tot} + [S]_{tot} + K_S)^2 - 4[E]_{tot}[S]_{tot}}\right]. \tag{5}$$

As mentioned before, in the case of α-chymotrypsin acylation is rate limiting for amide and anilide substrates (Fersht, 1985), i.e. $k_2 << k_3$, and it follows that [EP′] << [ES].

Therefore, [EP′] can be neglected in the enzyme's mass balance used to derive Eq. (5) for Scheme 1, i.e. $[E]_{tot} \cong [E] + [ES]$.

α-Chymotrypsin-Catalyzed Substrate Hydrolysis in the Vesicle System

The vesicle system is schematically illustrated in Fig. 1, showing one single vesicles of radius R_v, α-chymotrypsin which is entrapped inside the vesicle (E_{inside}), substrate S, and the two reaction products P_1 and P_2. The flux of S from the external bulk phase across the vesicle bilayer into the aqueous interior is assumed to follow Fick's first law of diffusion (Cevc, 1993; Stein, 1986). The batch balance for substrate in the bulk liquid is

$$\frac{d[S]_{outside}}{dt} = -\frac{P_S A([S]_{outside} - [S]_{inside})}{V_{outside}}, \qquad (6)$$

where $[S]_{outside}$ and $[S]_{inside}$, given in *M*, are the substrate concentration outside the vesicles at time *t* and the free substrate concentration inside the vesicles at time *t*, respectively. P_S is the permeability coefficient for S, given in cm/s, and *A* is the total vesicle surface area in the system, in cm^2; $V_{outside}$ is the exovesicular volume, in cm^3. The concentration of S inside the vesicles at time *t* can be calculated by applying a batch balance to the vesicles phase, which gives

$$\frac{d[S]_{tot,inside}}{dt} = \frac{P_S A([S]_{outside} - [S]_{inside})}{V_{inside}} - v \qquad (7)$$

with the initial conditions $[S]_{0,inside} = 0$ at $t = 0$ and where V_{inside} is the endovesicular volume of the system.

The transformation of S into P_1 and P_2 is described by the kinetics of Eq. (5), see above, which when applied to vesicular (inside) conditions becomes

$$v = \frac{k_2}{2}[([E]_{tot,inside} + [S]_{tot,inside} + K_S) - \sqrt{([E]_{tot,inside}+[S]_{tot,inside}+K_S)^2 - 4[E]_{tot,inside}[S]_{tot,inside}})]. \qquad (5')$$

Here, $[E]_{tot,inside}$ and $[S]_{tot,inside}$ are the total enzyme and substrate concentrations inside the vesicles, respectively.

For this vesicle–bulk phase batch system the total amount of product can be obtained at any time by the differences between the initial substrate concentration and the substrate concentration remaining in both phases at any time. This gives

$$[P]_{overall} = [S]_{0,overall} - \frac{V_{inside}[S]_{tot,inside} + V_{outside}[S]_{outside}}{V_{tot}}, \qquad (8)$$

where $[P]_{overall}$ and $[S]_{0,overall}$ are the overall concentration of one of the two products at time *t* and the concentration of S at $t = 0$, respectively. In the model used, the permeability of the spectrophotometrically measured product *p*-nitroaniline was also considered, even though its permeability coefficient P_P has no influence on the kinetics (with the assumption of negligible product inhibition). Therefore, P_P could be chosen freely to decrease calculation time.

RESULTS AND DISCUSSION

The aim of our work was to develop a general model for the kinetic behavior of water-soluble enzymes entrapped inside vesicles. We have attempted in particular to model the case of a two-phase (vesicle phase–bulk phase) batch reactor in which substrate is initially present only in the exovesicular bulk phase. For reaction to occur, the substrate molecules first have to be transferred from the bulk phase into the vesicular phase across the bilayer membrane, to reach the enzyme localized in the aqueous interior of the vesicles. The modeling of this microreactor system was applied for α-chymotrypsin-containing POPC vesicles to which the substrate Bz-Tyr-pNA initially added and during reaction was subsequently transferred into the vesicles.

Dynamic Simulation α-Chymotrypsin-Catalyzed Batch Reactions in the Absence of Vesicles

In the following, we will first show how Eq. (5) can be applied for the determination of k_{cat} and K_S from a single measurement in the absence of vesicles. In this case the software ModelMaker was used to fit experimental product concentration versus time data from a batch reactor. We then compare the values obtained for k_{cat} and K_S ($\cong K_M$) with the corresponding values from a classical enzyme kinetic analysis, based on initial velocity measurements at different substrate concentrations and utilizing the Michaelis–Menten equation, Eq. (2), and some of its well-known linearized representations (Fersht, 1985; Segel, 1975). The results are listed in Table I.

In a first test, we checked the reproducibility and the absolute values obtained for k_{cat} and K_S from a fit of experimental batch product concentration–time curves for a fixed set of enzyme and initial substrate concentrations (16.5 n*M* α-chymotrypsin and 123 μ*M* Suc-Ala-Ala-Pro-Phe-pNA), see Table IAa. Fitting for all 5 measurements gave values for k_{cat} between 33 and 41 s^{-1} and for K_S between 35 and 43 μ*M*. The mean values and standard deviations for this set of measurements were 37 ± 3 s^{-1} (k_{cat}) and 41 ± 3 μ*M* (K_S). For a comparison between measured values and the corresponding fitted [product]–time curve, see Fig. 3.

In a next series of batch reactor measurements, the initial concentration of substrate (again Suc-Ala-Ala-Pro-Phe-pNA) was varied from 21 to 98 μ*M* with either 6.3 or 16.5 n*M* α-chymotrypsin, and the corresponding [product]–time curves were fitted with Eq. (5). The mean values and standard deviations obtained from these eight measurements were 35 ± 5 s^{-1} and 44 ± 15 μ*M* for k_{cat} and K_S, respectively, see Table IAb. These values were in good agreement with those obtained from a classical Michaelis–Menten analysis from determinations of initial velocities at different

Table I. Kinetic characterization of α-chymotrypsin in aqueous solution at 25°C in the absence of vesicles. Substrate (S): Suc-Ala-Ala-Pro-Phe-pNA.

	k_{cat} (s^{-1})	K_S ($\cong K_M$) (μM)
(A) Determination by dynamic simulation using Eq. (5) kinetics		
(a) Enzyme and substrate concentrations fixed: $[\alpha\text{-chymotrypsin}]_{tot}$ = 16.5 n*M*; $[S]_0$ = 123 μM; 0.1 *M* Tris/HCl, pH 8, 10 m*M* $CaCl_2$		
Mean values and standard deviations from 5 measurements (as shown in Fig. 3)	37 ± 3	41 ± 3
(b) Enzyme and substrate concentrations varied: 0.1 *M* Tris/HCl, pH 8, 10 m*M* $CaCl_2$; $[\alpha\text{-chymotrypsin}]_{tot}$ either 6.3 or 16.5 n*M*; $[S]_0$ = 21–98 μM		
Mean values and standard deviations from 8 measurements	35 ± 5	44 ± 15
(B) Determination by using Eq. (2) and initial velocity data at different substrate concentrations: $[\alpha\text{-chymotrypsin}]_{tot}$ = 6.3 n*M*; 21 $\mu M \leqslant [S]_0 \leqslant$ 254 μM (8 concentrations); 0.1 *M* Tris/HCl, pH 8, 10m*M* $CaCl_2$		
Method		
Lineweaver–Burk	28	34
Eadie–Hofstee	28	34
Hanes	29	40
Eisenthal and Cornish–Bowden	29	44

(C) Literature values Conditions	k_{cat} (s^{-1})	K_M (μM)	Reference
0.1 *M* Tris/HCl, pH 7.8, 10 m*M* $CaCl_2$	45	43	DelMar et al., 1979
0.1 *M* Tris/HCl, pH 8, 10 m*M* $CaCl_2$	36	30	Bru and Walde, 1991
0.1 *M* Tris/HCl, pH 8	38	31	Mao and Walde, 1991

substrate concentrations (21–254 μM), at a fixed amount of α-chymotrypsin (6.3 n*M*), and using one of the known graphical methods, see Table IB. For comparison, literature values are listed in Table IC.

From all the test measurements in the absence of vesicles we concluded that the general Eq. (5) can successfully be applied for determining the characteristic parameters k_{cat} and K_S ($\cong K_M$) for α-chymotrypsin from single measurements at known initial total substrate and total enzyme concentrations using amide and anilide substrates.

For Bz-Tyr-pNA hydrolysis, k_{cat} and K_S were determined by fitting the mean of three batch product concentration–time curves with Eq. (5), see Table II. Differences in the kinetic constants with respect to published values are most likely due to considerable differences in the experimental conditions used.

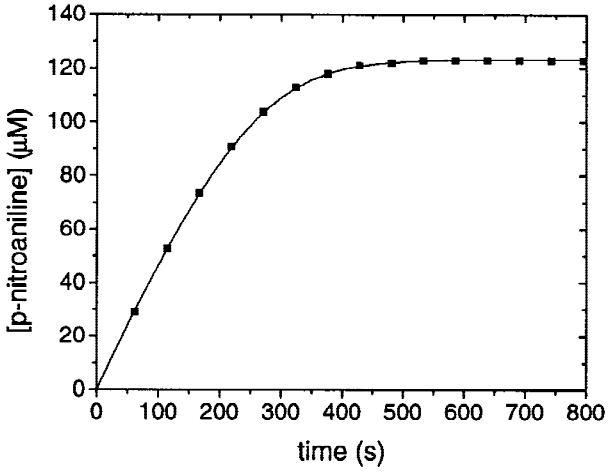

Figure 3. [Product]–time curve for the α-chymotrypsin catalyzed hydrolysis of Suc-Ala-Ala-Pro-Phe-pNA in the absence of vesicles; [α-chymotrypsin] = 16.5 n*M*, $[\text{Suc-Ala-Ala-Pro-Phe-pNA}]_0$ = 123 μM, 0.1 *M* Tris/HCl, pH 8, 10 m*M* $CaCl_2$, 25°C. The formation of *p*-nitroaniline is plotted as a function of reaction time. Filled squares are the experimental points used for the simulation. The solid line is the calculated curve obtained from the simulation with ''ModelMaker'' using Eq. (5). Results from the simultaneous fit for K_s and k_{cat}: K_S = 42 μM; k_{cat} = 41 s^{-1}.

Characterization of α-Chymotrypsin-Containing Vesicles

Since the modeling of our kinetic measurements with the vesicle system required the knowledge of vesicle size and phospholipid and enzyme concentrations, we have carried out a corresponding analysis of the reaction system, involving a variety of assumptions as outlined in the following.

The size of the α-chymotrypsin-containing vesicles was determined by dynamic light scattering measurements at different scattering angles. The hydrodynamic radius (R_H) obtained at 60, 90, and 120° were 64.2 ± 0.7, 63.6 ± 0.7, and 62.6 ± 1.0 nm, respectively. This insensitivity to the scattering angle indicated that the vesicles prepared were rather monodisperse, in analogy to what has been observed before with similarly sized, extruded POPC vesicles in the absence of α-chymotrypsin (Dorovska-Taran et al., 1996). Electron

Table II. Kinetic characterization of α-chymotrypsin in aqueous solution in the absence of vesicles; Substrate (S) is Bz-Tyr-pNA.

(A) Determination by dynamic simulation, using Eq. (5) kinetics: $[\alpha\text{-chymotrypsin}]_{tot} = 386$ n*M*; $[S]_0 = 105$ μ*M*; 0.05 *M* Tris/HCl, pH 8, 7% (v/v) dimethyl sulfoxide, 25°C

Method	$k_{cat}(s^{-1})$	$K_s(\cong K_M)(\mu M)$
Fit of a mean [product]–time curve obtained from 3 measurements	0.17	69

(B) Literature values

Conditions	$k_{cat}(s^{-1})$	$K_M(\mu M)$	Reference
36 m*M* Tris/HCl, pH 8, 45 m*M* $CaCl_2$, 9.7% (v/v) acetone, 35°C	0.88	340	Bundy et al., 1963

micrographs obtained either by the freeze-fracture technique or by cryoimmobilization confirmed a rather narrow size distribution (Fig. 4). Furthermore, most of the vesicles appeared unilamellar in the electron micrographs; this is in agreement with literature data reported for phosphatidylcholine vesicles extruded through polycarbonate membranes with 100 nm pores (Mayer et al., 1986). For the modeling described below, we have assumed unilamellarity and an uniform spherical vesicle size with a constant outer radius of 63.5 nm as indicated in Table III, where additionally, the concentrations of POPC and α-chymotrypsin are given. With the assumption that all enzyme molecules were equally distributed among all the vesicles, one can calculate that each vesicles contained 87 active α-chymotrypsin molecules. The calculated concentration of α-chymotrypsin inside every vesicle was 147 μ*M*, see Table III. With the assumption that for Bz-Tyr-pNA hydrolysis, k_{cat} and K_S for α-chymotrypsin in the aqueous pool of the vesicles are the same as the corresponding values in bulk buffer solution, we proceeded to the computer modeling of the vesicular system.

Dynamic Simulation of α-Chymotrypsin-Catalyzed Batch Reactions in the Vesicle System

The filled squares in Fig. 5 are experimental data obtained from measurements in 50 m*M* Tris/HCl buffer (pH 8) with α-chymotrypsin-containing vesicles to which the substrate Bz-Tyr-pNA initially only externally present. The conditions of the experiment are listed in Table III. In order to avoid any interference of the measurements with leaked α-chymotrypsin or with α-chymotrypsin which could be adsorbed onto the external surface of the vesicles, the α-chymotrypsin inhibitor protein BPTI ($M_r \sim 6{,}500$) was added to an overall concentration of 5 μ*M* (Walde and Marzetta, 1998). Estimations from comparative determinations of initial velocity measurements with Suc-Ala-Ala-Pro-Phe-pNA with and without 40 m*M* sodium cholate in the absence of inhibitor showed that in our preparations only about 0.6% of the total α-chymotrypsin eluting with the vesicles (pooled fractions of peak 1 in Fig. 2) was exovesicular.

The experimental data were fitted for one single parameter, $P_{Bz\text{-}Tyr\text{-}pNA}$, the permeability coefficient of the substrate, by using basically Eq. (6) and (7) and 69 μ*M* for K_S ($\cong K_M$) and 0.17 s^{-1} for k_{cat} ($\cong k_{cat}$) (see Table IIA). The fitted curve is shown as solid line in Fig. 4. The agreement between the experimental values and the simulated curve was excellent, and we obtained a value for the permeability coefficient for Bz-Tyr-pNA ($P_{Bz\text{-}Tyr\text{-}pNA}$) with respect to the POPC bilayer of 2.45×10^{-7} cm/s.

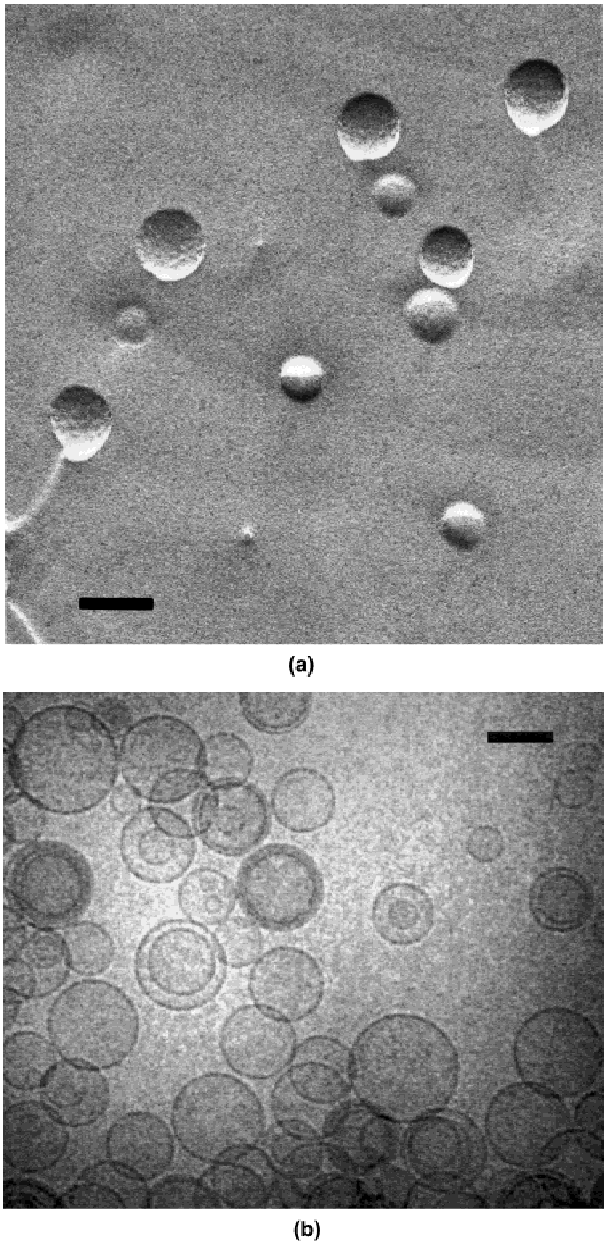

Figure 4. Freeze–fracture (a) and cryoimmobilized (b) electron micrographs of POPC vesicle preparations containing entrapped α-chymotrypsin: Length of the bar, 100 nm.

Table III. Characteristic properties of the α-chymotrypsin-containing vesicle sample used in this study.[a]

[POPC]	86 μ*M*
$[\alpha\text{-Chymotrypsin}]_{overall}$	56 n*M*
Mean hydrodynamic vesicle radius (R_H)	63.5 nm
Mean geometric vesicle radius used ($R_v = R_H - 1.9$ nm)	61.6 nm
Number of POPC molecules per vesicle	132,600
Volume of one vesicle	9.8×10^{-22} m^3
Percentage of volume trapped by the vesicles	0.038%
[Vesicle]	0.65 n*M*
Mean number of α-chymotrypsin molecules per vesicle	87
$[\alpha\text{-Chymotrypsin}]_{vesicle\ interior} = [\alpha\text{-chymotrypsin}]_{inside}$	147 μ*M*
$[\text{Bz-Tyr-pNA}]_{0,exovesicular} = [\text{Bz-Tyr-pNA}]_{0,outside}$ ($\approx[\text{Bz-Tyr-pNA}]_{0,overall}$)	104 μ*M*

[a]Unless otherwise indicated, all concentrations refer to overall concentrations as used in the kinetic measurements which were modeled. For the calculations, monodispersity, unilamellarity and a spherical vesicle shape were considered (see text). Furthermore, a bilayer thickness of 3.7 nm and a mean POPC head group area of 0.72 nm^2 were taken into account (Huang and Mason, 1978; Cornell et al., 1980). The concentrations of the substrate (Bz-Tyr-pNA) are given for $t = 0$.

CONCLUDING REMARKS

Apart from a few experimental papers (Madeira, 1977; Sada et al., 1988; Annesini et al., 1992; see also Walde, 1996) and a theoretical approach (Cioci and Lavecchia, 1993, 1995), our modeling is a first attempt to quantify enzymatic reactions occurring in the aqueous interior of vesicles.

Although quite successfully applied in the present work, one has to admit that one limitation in the use of single [product]–time curves for determining kinetic constants for enzyme-catalyzed reactions is the requirement of following the reaction until equilibrium (or almost equilibrium). This may not always be possible due to unreasonably high reaction times required (e.g. at low enzyme concentrations or for low k_{cat} or high K_M values). Furthermore, the use of high substrate concentrations may cause analytical problems (e.g., high absorbance in the case of chromogenic substrates or products, respectively). Additionally, possible inhibitions caused by high concentrations of reaction products which remain trapped inside the vesicles (e.g., charged products) were not included in the present treatment. This could, however, in principle be done if required.

Despite these limitations, our modeling and parameter estimation procedure allowed not only the quantification of the substrate permeability in the vesicle system used, but also provided an insight into the changes of substrate concentrations inside and outside of the vesicles, as well as changes in the concentration of the enzyme–substrate complex inside the vesicles ($[ES]_{inside}$), see Fig. 6. All these values would be rather difficult to determine experimentally.

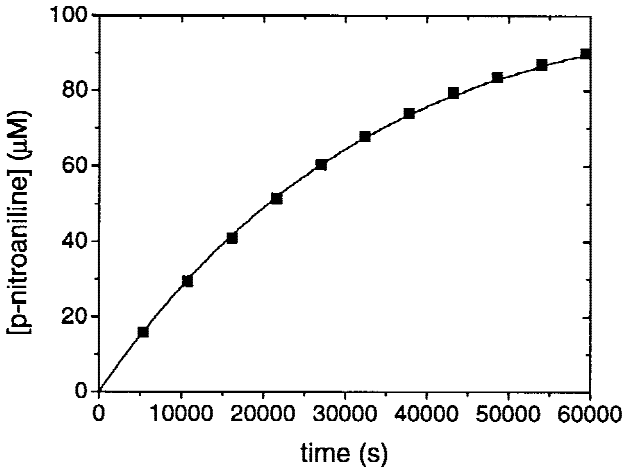

Figure 5. [Product]–time curve for the α-chymotrypsin catalyzed hydrolysis of Bz-Tyr-pNA added externally to POPC vesicles containing entrapped α-chymotrypsin. For the experimental conditions, see Table III. The formation of *p*-nitroaniline (measured overall) is plotted as a function of reaction time. Filled squares are the experimental points obtained in the presence of 5 μ*M* BPTI (overall) and used for the simulation. The concentration of dimethyl sulfoxide was 7% (v/v). The solid line is the fitted curve obtained with ''ModelMaker'' and basically using Eqs. (6) and (7). Results from the fit for the substrate permeability coefficient using k_{cat} and K_S from Table IIA: $P_{Bz\text{-}Tyr\text{-}pNA} = 2.45 \times 10^{-7}$ cm/s.

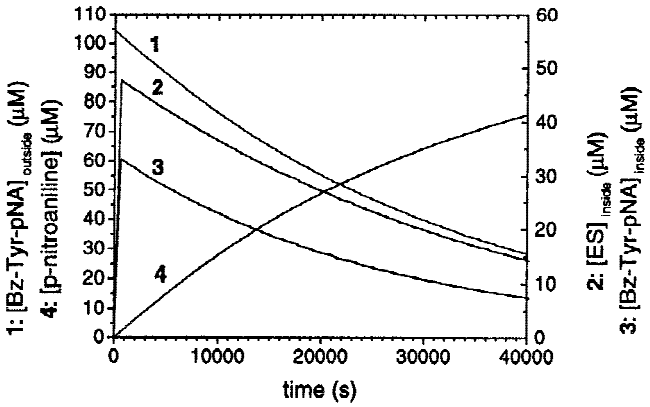

Figure 6. Calculation of the concentration–time profiles for the α-chymotrypsin-catalyzed hydrolysis of Bz-Tyr-pNA in the vesicular system. Using the values obtained from the simulation of the experimental $[p\text{-nitroaniline}]_{overall}$–time curve (4), the following concentration–time profiles were calculated: [Bz-Tyr-pNA] inside the vesicles (3), [Bz-Tyr-*p*-nitroaniline] outside the vesicles (1), and the concentration of the enzyme–substrate complex, [ES], inside the vesicles (2).

The authors thank Anna Suter from Pharma Research at Novartis International Ltd., Basel, Switzerland, for the POPC sample. For the electron microscopy analysis carried out in the Laboratory for Electron Microscopy I of the ETH, we also thank Michaela Wessicken (freeze–fracture method) and Nathalie Berclaz (cryoimmobilization).

Supplementary Material

The listing of the ''model definition'' used can be obtained as supplementary material from the authors.

References

Annesini MC, DiGiulio A, DiMarzio L, Finazzi-Agrò A, Mossa G. 1992. Diffusion and catalysis processes in unilamellar liposomes. J Liposome Res 2:455–467.

Anzai K, Yoshida M, Kirino Y. 1990. Change in intravesicular volume of liposomes by freeze–thaw treatment as studied by the ESR stopped-flow technique. Biochim Biophys Acta 1021:21–26.

Bangham AD, Standish MM, Watkins JC. 1965. Diffusion of univalent ions across the lamellae of swollen phospholipids. J Mol Biol 13:238–252.

Bru R, Walde P. 1991. Product inhibition of α-chymotrypsin in reverse micelles. Eur J Biochem 199:95–103.

Bundy HF. 1963. Chymotrypsin-catalyzed hydrolysis of N-acetyl- and N-benzoyl-L-tyrosine p-nitroanilides. Arch Biochem Biophys 102: 416–422.

Cevc G. 1993. Solute transport across bilayers. In: Cevc G (ed.), Phospholipids handbook. New York: Marcel Dekker, Inc. p 639–661.

Cioci F, Lavecchia R. 1993. Urease-loaded liposomes as detoxifying microreactors: Effect of ammonia accumulation on enzyme kinetics. J Liposome Res 3:725–735.

Cioci F, Lavecchia R. 1995. Carrier-mediated transport phenomena in enzyme-loaded liposomes. J Liposome Res 5:291–309.

Cornell BA, Middlehurst J, Separovic F. 1980. The molecular packing and stability within highly curved phospholipid bilayers. Biochim Biophys Acta 598:405–410.

DelMar EG, Largman C, Brodrick JW, Geokas MC. 1979. A sensitive new substrate for chymotrypsin. Anal Biochem 99:316–320.

Dorovska-Taran V, Wick R, Walde P. 1996. A ^{1}H nuclear magnetic resonance method for investigating the phospholipase D-catalyzed hydolysis of phosphatidylcholine in liposomes. Anal Biochem 240:37–47.

Egelhaaf SU, Wehrli E, Müller M, Adrian M, Schurtenberger P. 1996. Determination of the size distribution of lecithin liposomes: A comparative study using freeze–fracture, cryoelectron microscopy and dynamic light scattering. J Microsc 184:214–228.

Fersht A. 1985. Enzyme structure and mechanism. 2nd edition. New York: WH Freeman and Company.

Hope MJ, Nayar R, Mayer LD, Cullis PR. 1993. Reduction of liposome size and preparation of unilamellar vesicles by extrusion techniques, In: Gregoriadis G, editor. Liposome technology, Vol. 1. 2nd edition. Boca Raton, FL: CRC Press. p 123–139.

Huang C, Mason JT. 1978. Geometric packing constraints in egg phosphatidylcholine vesicles. Proc Natl Acad Sci 75:308–310.

Keleti T. 1986. Basic enzyme kinetics. Budapest: Akadémiai Kiadó.

Lynch DV, Steponkus PL. 1989. Lyotropic phase behavior of unsaturated phosphatidylcholine species: Relevance to the mechanism of plasma membrane destabilization and freezing injury. Biochim Biophys Acta 984:267–272.

Madeira VMC. 1977. Incorporation of urease into liposomes. Biochim Biophys Acta 499:202–211.

Mao Q, Walde P. 1991. Substrate effects on the enzymatic activity of α-chymotrypsin in reverse micelles. Biochem Biophys Res Commun 178:1105–1112.

Mayer LD, Hope MJ, Cullis PR. 1986. Vesicles of variable sizes produced by a rapid extrusion procedure. Biochim Biophys Acta 858:161–168.

Mayer LD, Hope MJ, Cullis PR, Janoff AS. 1985. Solute distributions and trapping efficiencies observed in freeze–thawed multilamellar vesicles. Biochim Biophys Acta 817:193–196.

Müller M, Meister N, Moor H. 1980. Freezing in a propane jet and its application in freeze–fracturing. Mikroskopie (Wien) 36:129–140.

Naoi M, Naoi M, Shimizu T, Malviya AN, Yagi K. 1977. Permeability of amino acids into liposomes. Biochim Biophys Acta 471:305–310.

Papahadjopoulos D, Kimelberg HK. 1974. Phospholipid vesicles (liposomes) as models for biological membranes: Their properties and interactions with cholesterol and proteins. Prog Surf Sci 4:141–232.

Rosenberg MF, Jones, MN, Vadgama PM. 1991. A liposomal enzyme electrode for measuring glucose. Biochim Biophys Acta 1115: 157–165.

Sada E, Katho S, Terashima M, Tsukiyama K. 1988. Entrapment of an ion-dependent enzyme into reverse-phase evaporation vesicles. Biotechnol Bioeng 32:826–830.

Scheper T. 1990. Enzyme immobilization in liquid surfactant membrane systems. Adv Drug Delivery Rev 4:209–231.

Schonbaum GR, Zerner B, Bender ML. 1961. The spectrophotometric determination of the operational normality of an α-chymotrypsin solution. J Biol Chem 236:2930–2935.

Segel IH. 1975. Enzyme kinetics. New York: John Wiley & Sons, Inc.

Stein WD. 1986. Transport and diffusion across cell membranes. Orlando, FL: Academic Press, Inc.

Stewart JCM. 1980. Colorimetric determination of phospholipids with ammonium ferrothiocyanate. Anal Biochem 104:10–14.

Torchilin VP. 1987. Immobilised enzymes as drugs. Adv. Drug Delivery Rev 1:41–86.

Walde P. 1996. Enzymatic reactions in liposomes. Curr Opin Colloid Interface Sci 1:638–644.

Walde P, Marzetta B. 1998. Bilayer permeability-based substrate selectivity of an enzyme in liposomes. Biotechnol Bioeng 57:216–219.